

Changes in Modal Parameters and Performance of a Prestressed Concrete Bridge under Step-by-step Loading

C.W. Kim¹, Y. Kondo², G. Hayashi³ and Y. Oshima⁴

¹ Department of Civil & Earth Resources Engineering, Graduate School of Engineering, Kyoto University, Kyoto, Japan. Email: kim.chulwoo.5u@kyoto-u.ac.jp

² TEPCO, Tokyo, Japan (formerly a graduate student at Kyoto University, Kyoto, Japan). Email: k.18-iki-1220@ezweb.ne.jp

³ Urban Engineering, Graduate School of Engineering, Osaka City University, Osaka, Japan (formerly a researcher at Kyoto University, Kyoto, Japan). Email: hayashi-g@osaka-cu.ac.jp

⁴ Nakano Corporation, Tokyo, Japan (formerly a senior researcher at Public Works Research Institute, Japan). Email: oshima_yoshinobu@wave-nakano.co.jp

Abstract: This study discusses a bridge collapse test under static loading on a real prestressed concrete (PSC) bridge. In the static loading test, step-by-step loading until failure were considered. Forced vibration test was also carried out along with the static loading test to investigate how changes in performance of the PSC bridge affect modal properties of the bridge. The structural performance feature that makes use of the potential energy and energy dissipation in each load step is calculated from load-displacement relation and is adopted to estimate the structural performance of the PC bridge. Observations showed that the 1st bending frequency was little connection to the structural performance feature. On the other hand, strong relationships between the 2nd bending modal frequency and the level of structural performance was observed. This demonstrates the usefulness of the 2nd bending mode in vibration-based bridge health monitoring for the PSC bridge.

Keywords: field experiment, prestressed concrete bridge, static-loading test, structural health monitoring, vibration monitoring

1. Introduction

Prestressed concrete (PSC) girder bridges have been constructed in Japan since 1970s, and various damages due to deterioration such as corrosion of prestressing (PS) tendons have been reported. Visual inspection is one of the most popular approaches to assess integrity of the PSC bridge although many methods are proposed to evaluate soundness of bridges. For the PSC bridge, the compressive stress introduced by the PS tendon cancels out the tensile stress caused by the external load, and the crack occurs when the tensile stress reaches crack strength. In other words, occurrence of cracks on the PSC girder is associated with higher possibility of excessive stresses and less margin of strength in the PSC bridge.

In addition, damages caused by different sources lead to different effects on load resisting capacity of the PSC bridge, and it is desirable to evaluate soundness of the PSC bridge not only from external appearance but also from a physical index. Vibration-based structural health monitoring (SHM) thus has been developed as an approach providing a physical index on soundness of bridges. Natural frequencies from deteriorated concrete girders have shown to be a sensitive feature for the strength reduction when evaluating the residual strength in bridges with 50 years of service life (Kato and Shimada 1986). At the same time, it rises the likelihood of using natural frequencies as a feature to be monitored in order to estimate the structural reliability (Quattorone et al. 2012).

Literatures also show that the modal damping ratio can be a damage sensitive feature for reinforced and prestressed concrete structures. Moreover, researches indicate that a trend of getting higher value of modal damping ratios with the age of the bridges could be a sign of possible deterioration, which is a strong reason to investigate the relationship between damping parameter

and degree of damage (Dammika et al. 2015). However, more evidences are required to validate residual strength models of deteriorating bridges (Cavell and Waldron 2001) and to prove the link between structural resistance and information for SHM (Dilena et al. 2011).

Damage in structures is interpreted as a decay of its mechanical properties, or a decrease in stiffness. However, the tendency of changes in natural frequencies to the development of damage shows an abnormal increase/decrease from one configuration to another even experimentally (Dilena and Morassi 2011). Structural analysis is a good option to examine unexpected tendency observed from the field experiment once inconsistencies between experiment and theoretical models are clarified (Udwadia 2005).

The natural frequency of the first bending mode showed to rapid decaying tendency, but little change in the damping was observed in the failure process of a PSC bridge (Kato and Shimada 1986). It was noticed that the small changes in modal parameters, regardless of the large presence of cracks in concrete structures, might be due to the cracks closing by effective prestressing when the structure is unloaded. Theoretically decrease of prestressing force increases the natural frequencies in a concrete element because a reduction in the axial compressive load would stiffen the element. An opposite trend was also observed in a PSC bridge (Saiidi et al. 1994) where the frequencies showed a small decrement after the decrease of prestressing force. Moreover, it is known that no substantial change was detected in the modal parameters after cutting PS tendons at a specific location of a PSC bridge (Döhler et al. 2014). However, few researches have been investigated relationship between changes in frequencies and structural performance of actual PSC bridges.

This study aims to examine changes in load resistance capacity and modal parameters of an actual PSC girder bridge through a bridge collapse-test. In the static loading test, several loading and unloading levels until failure were considered. The forced vibration test was carried out along with the static loading test in order to estimate the relationships between modal parameters and structural performance. Finite element analysis was also conducted to discuss the relationship between structural performance and modal properties of the PSC bridge in detail.

2. Target bridge

The target bridge and static loading device are shown in Figs. 1 and 2. The bridge is a five-span simply supported PSC bridge with four main PSC girders. The length of each span is 35.6m and the width is 7.2m. 12 pairs of steel strand ($12\phi*7$) were utilized as a PS tendon for each girder. The bridge is about 170m away from the coast line and had been operated more than 50 years since its construction. Therefore, chloride attack to the main girder was significant, and cracks of the main girder caused by corrosion of the internal steel rebar and spalling of the concrete were observed by visual inspection. Figure 3 shows the damage location map of the bridge obtained from the periodic inspection before the experiment. Damage was distributed throughout the span, and exposure of the reinforcing bar due to concrete peeling was observed at three locations. Considering the inspection result, reduced load carrying capacity was expected.

3. Field experiment

3.1 Static loading test

The static load test was carried out utilizing two 3000kN center hole type hydraulic jacks installed on the loading beam with a loading block. Fig. 2 shows the loading device installed on the PSC bridge. The load was applied statically and monotonously. As a reaction device for the static loading, two tendons having a loading capacity of 2500kN for each are anchored to the underground sandstone layer. The applying load was monitored by the load cell and the jack stroke was monitored during loading. The loading point was set at the span center of the G1 girder (see Fig. 2 and Fig. 4). Sensor deployment map is shown in Fig. 4. The vertical displacement of each observation point was measured by displacement transducers installed under the girder. Moreover, the longitudinal displacements at both ends of the G1 girder were also measured.

The static loading progress and vibration test stage are shown in Fig. 5 in which “Stage n ” indicates the time of the vibration test. The static loading and vibration tests were conducted over three days. Five stages of the static loading test (Loading-1 to Loading-5) until fracture of the guard rail were considered. Loading-1 is the scenario loaded up to 600kN which induces bending cracks to the main girder. Loading-2 is the scenario loaded up to 1200kN which is the yield load of the reinforcing bar (hereafter, rebar). In Loading-3, as with Loading-2, static load of 1200kN was applied again but the loading was kept for about two hours. Loading-4 is the scenario loaded up to 2400kN which is the failure load predicted in a preliminary structural analysis. Loading-5 is loaded up to

3200kN which leads to fracture of the guiderail. It is noted that the load resisting capacity of the PSC bridge was about 1.3 times larger than the analytical ones. The static loading test demonstrated that the damages and deterioration during the service period have hardly affected bending performance of the bridge.



Figure 1. Target bridge.



Figure 2. Loading device.

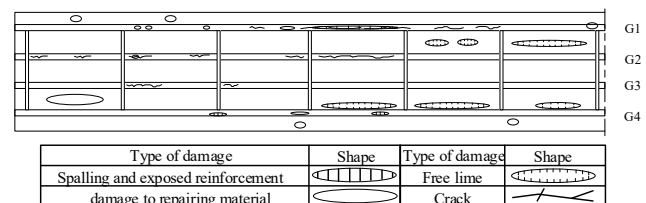


Figure 3. Damage location map.

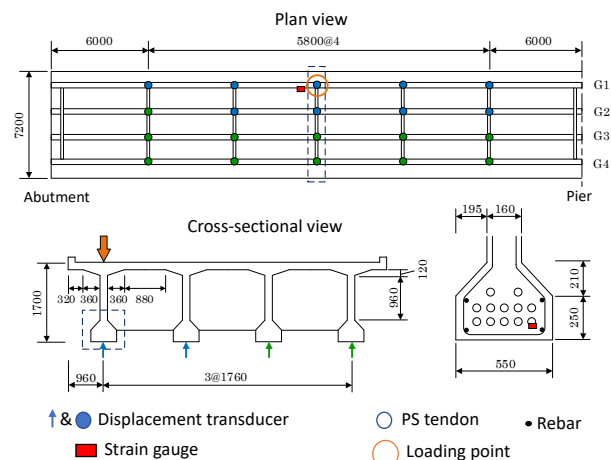


Figure 4. Sensor location map (Unit: mm).

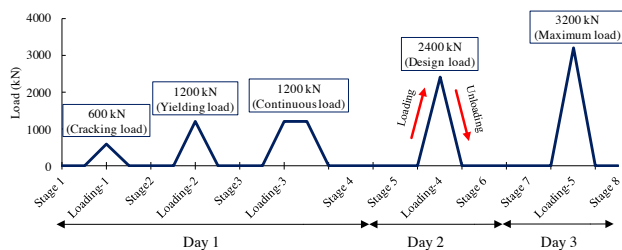


Figure 5. Static loading process and vibration test stages.

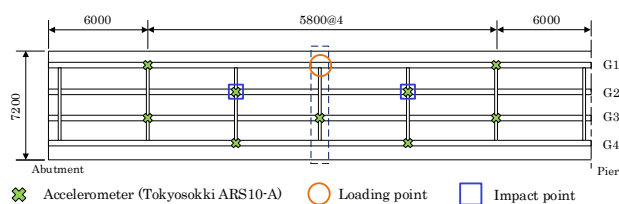


Figure 6. Location of impact points and accelerometers (Unit: mm).

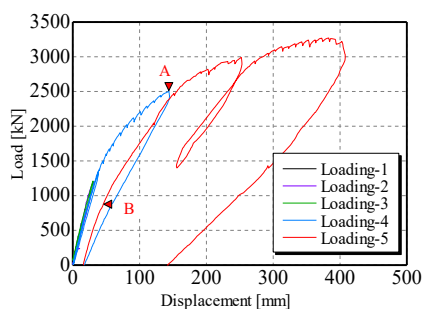


Figure 7. Load-vertical displacement curve (span center of G1 girder).

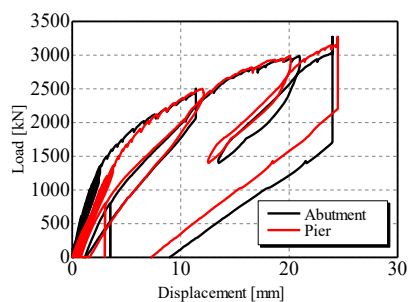


Figure 8. Load-longitudinal displacement curve (on pier and abutment of G1 girder).

3.2 Dynamic test

An impact test utilizing a hammer was conducted under unloaded situation after each static loading (see Fig. 5) to examine changes in the dynamic properties of the bridge with different health conditions. As can be seen in Fig. 5, Stage 1 is the initial state before the static load test. Stage 2 is the unloaded state after Loading-1 (600kN), and Stage 3 is the unloaded state after Loading-2 (1200kN). Stage 4 is the unloaded state after Loading-3 which is the state of being loaded by 1200kN for about 2 hours. Stage 5 indicates the state that the bridge was left overnight after

Stage 4. Stage 6 is the unloaded state after Loading-4 (2400kN), and Stage 7 is the state when the bridge is left overnight after Stage 6. Finally, Stage 8 is the unloaded state of Loading-5 (3200kN).

The vibrations induced by the impact were measured utilizing strain gauge type accelerometers (ARS10-A, Tokyo Sokki). The location of accelerometers and hitting points are shown in Fig. 6. The total hitting times was 40 times per each stage.

4. Structural Performance of PSC Bridge

4.1 Load-displacement Relation

The load-vertical displacement curve observed at the span center of the G1 girder is shown in Fig. 7, in which no clear residual displacement is observed until Loading-3. It indicates that the bridge behavior was elastic until Loading-3. At Loading-4, the bridge was loaded up to 2500kN (designed failure load) and unloaded, this loading step resulted in the residual displacement of around 16mm. When the bridge is reloaded (Loading-5), the load-vertical displacement curve traces the unloading points (point A in Fig. 7), which indicates enough restoration performance. The gradient of reloading under Loading-5 is almost the same as that of the Loading-1 to Loading-4 until the tensile stress occurs at the lower edge of the PSC girder (point B in Fig. 7). This indicates that the prestressing force remains and makes the entire section keep effective. Therefore, it can be said that the vibration characteristics would be hardly changed as the initial stiffness keeps almost constant through Stage 1 to Stage 5. Relationships between structural performance and vibration characteristics are discussed in Section 4.4.

The load-longitudinal displacement curves observed at the supports of the G1 girder are shown in Fig. 8. It shows that the longitudinal displacements at both sides differ at the lower loading level (smaller than 1500kN). While the displacements reached same level at the higher load level (greater than 2000kN). This indicates that the behaviours of supports vary according to the load level.

4.2 Energy-based structural performance feature

A structural performance feature is introduced to normalize bending performance of the PSC bridge. The structural performance feature is estimated utilizing the potential energy and energy dissipation in each load step of the static loading test. Eq. (1) shows the structural performance feature (hereafter, performance feature) at loading- n ($n = 1, 2, \dots, 5$) with function of the energy dissipation (ΔW) and the potential energy (W). The energy dissipation (ΔW) and the potential energy (W) are explained in Fig. 9.

$$Z = \left(1 - \frac{\Delta W}{W}\right) \times 100 (\%) \quad (1)$$

When the PSC bridge behaves elastically and no damage occurs, the energy dissipation would be zero and the performance remains in 100%. On the contrary, if damage is introduced or the beam reaches its plastic range, the energy dissipation occurs, and the performance feature would show lower value than 100%. Fig. 10 shows the change in the performance with respect to each stage. It

can be seen that the performance feature Z has been drastically decreased when the static load reached cracking load (compare Z under st.1 and st. 2 in Fig. 10), design load (compare Z under st.4 and st. 6 in Fig. 10) and maximum load (compare Z under st.6 and st. 8 in Fig. 10).

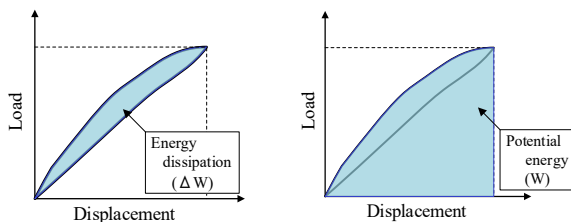
4.3 Modal parameters

Modal parameters of the PSC bridge such as natural frequency and damping ratio are identified from the vibration data. However, for the damping ratio, it was hard to observe obvious changes under step-by-step loading except the final loading that caused failure of guiderail and damping ratio increase. It is noted, however, the pattern with respect to each stage showed reverse pattern with those of frequencies.

This study thus focuses on the identified frequency as a representative dynamic property. Changes in identified frequencies for the 1st and 2nd bending modes are plotted in Fig. 11, which shows that the frequency for the 2nd bending mode resulted in stronger relationship with structural integrity. Similar observations are reported in (Luna Vera et al. 2020). Changes in mode shapes are shown in Fig. 12, but it was hard to observe a pattern. Moreover, the change in MAC values are too small to be utilized in damage detection except for the failure state.

4.4 Structural performance feature vs. frequency

The relationship between residual displacement and bending frequency are investigated utilizing residual displacement area shown in Fig.13(a). It is observed that a strong correlation exists between changes in residual displacement area and changes in bending frequencies as shown in Fig. 13(b) and (c). Therefore, changes in the performance feature Z and bending frequencies are investigated, and are shown in Fig. 14. The dotted line shows a linear regression between frequency and performance feature from Stage 1 to Stage 7. Stage 8 was not considered to the regression since Stage 8 is close to the ultimate condition which rarely occurs in real bridge monitoring. From the linear regression curve, a strong correlation was observed between the 2nd bending modal frequency and the performance feature.



(a) Energy dissipation (b) Potential energy
 Figure 9. Energy dissipation and potential energy.

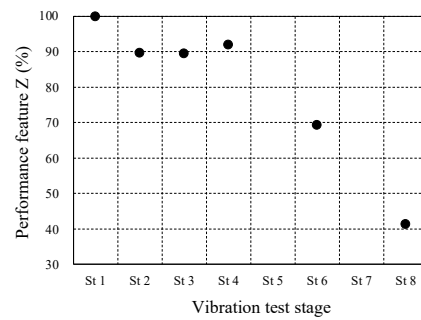
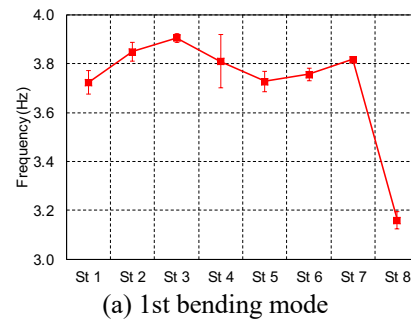
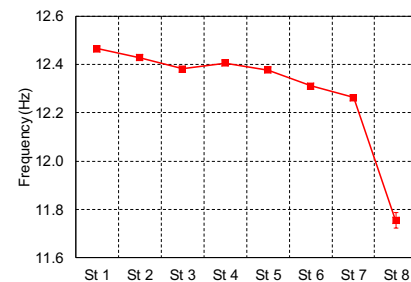


Figure 10. Change in performance feature.

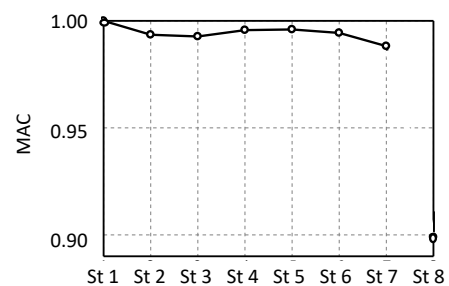


(a) 1st bending mode

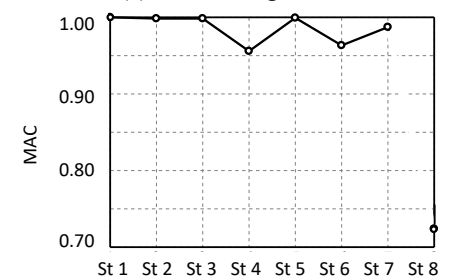


(b) 2nd bending mode

Figure 11. Change in bending modal frequency.

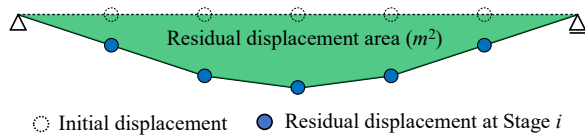


(a) 1st bending mode

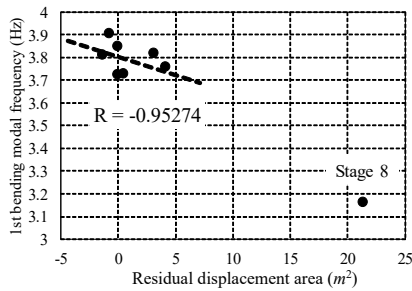


(b) 2nd bending mode

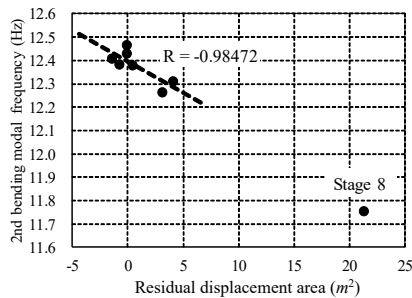
Figure 12. Change in MAC values.



(a) Concept of residual displacement area

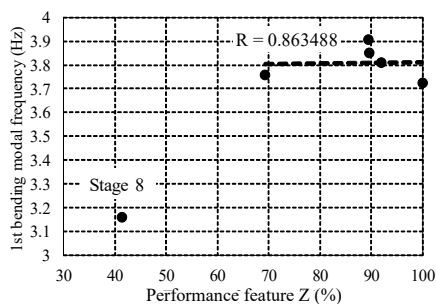


(b) 1st bending mode

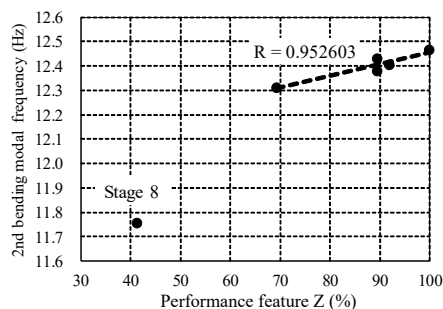


(c) 2nd bending mode

Figure 13. Residual displacement area vs. Normalized frequency.



(a) 1st bending mode



(b) 2nd bending mode

Figure 14. Performance feature vs. frequency.

Table 1. Horizontal spring constant and eigen frequencies.

Static load F_s (kN)	Analysis		Experiment
	$0 \leq F_s \leq 600$	$600 < F_s$	
Spring constant at Abutment (N/m)	1.77×10^8	2.27×10^8	-
Spring constant at Pier (N/m)	3.55×10^8	2.79×10^8	-
Rotational spring (N/rad)	1.0×10^9		-
1st bending modal freq. (Hz)	3.78	3.79	3.75
2nd bending modal freq. (Hz)	11.3	11.3	12.48

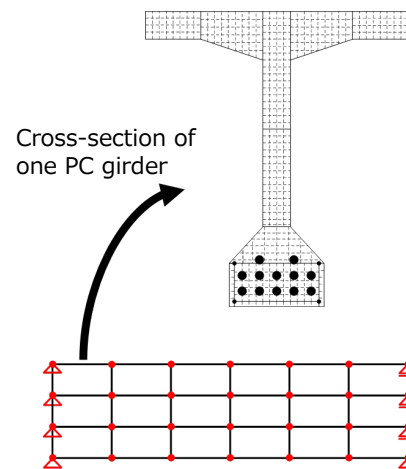


Figure 15. FE model of the target bridge with mesh for fiber model.

5. Finite element analysis (FEA)

Finite element (FE) analysis was conducted to discuss the relationship between structural performance and modal properties of the PSC bridge in detail. The FE model for the target bridge is constructed by the fibre model which is a kind of beam models and can easily grasp the nonlinear behaviour of members. Fig. 15 shows the FE model of the target bridge. Concrete deck, main girders and guiderail were modelled with the fibre model. Cross beams were modelled with elastic beam and the pavement were modelled with shell element. All elements were rigidly connected. Based on the periodic inspection documents, Young's modulus of steel and concrete were assumed as 200 GPa and 40 GPa, respectively.

The horizontal springs were introduced to the bearings as the field test showed that both sides of the G1 girder moved in the longitudinal direction. The spring constants were estimated utilizing the measured longitudinal displacements. The bilinear horizontal springs and rotational spring were modeled in the FE model following the bi-linear behaviour of the longitudinal displacements. The spring constant of the rotational spring was decided 1.0×10^9 N/rad by a sensitivity analysis.

Eigenvalue analysis was conducted considering each spring constant. The 1st and 2nd bending modal natural frequencies obtained from the experiment were 3.72Hz and 12.46Hz respectively, and FEA considering the rotational spring resulted in comparable frequencies with the experimental ones as shown in Table 1.

In order to discuss the non-linear behavior of the model, the pushover analysis was conducted up to the same displacement as the Loading-4. Fig.16 shows the load-displacement curves from the experiment and FEA. From Fig.16, there is a large difference in the degree of the plasticity although the eigen frequencies were comparable with the experimental ones.

The similar loading step as in the experiment is considered in FEA, and the relationship between the performance feature and the normalized frequency is investigated. The normalized frequency is calculated by dividing the observed frequency at each vibration test stage by the frequency before the static loading test. When the bridge is unloaded after each loading step, eigenvalue analysis is conducted to obtain analytical natural frequencies of the bridge. Fig. 17 shows the comparison between performance feature and normalized frequency obtained from the analysis. It shows that changes in the energy and frequency obtained from the experiment for the 1st bending mode was not well simulated in comparison with Fig.14(a). While the 2nd bending mode showed a similar trend with experiment.

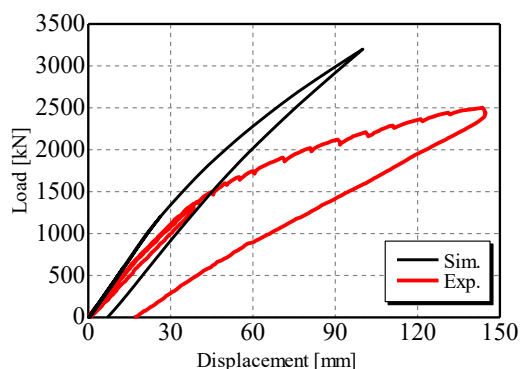


Fig. 16. Load vs. displacement curve.

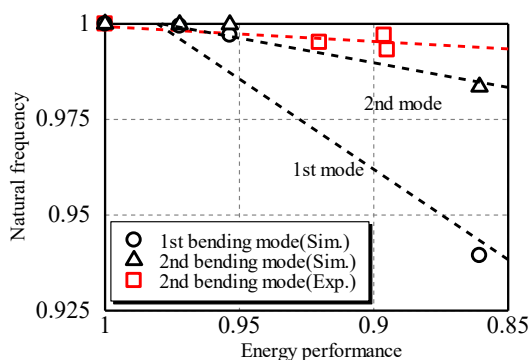


Fig. 17. Performance feature vs. normalized frequency.

6. Conclusions

This study investigates the relationship between bridge performance and modal frequencies through a bridge collapse-test. Finite element analysis was also conducted to discuss the relationship. From the experiment, the 2nd bending modal frequency showed stronger correlation with the structural performance feature than the 1st bending mode. This indicates the usefulness of the 2nd bending mode in vibration-based bridge health monitoring of the PSC bridge. However, the relationship obtained from the experiment is not well reproduced by the analysis, which is remaining tasks for future study. Whilst the 2nd bending mode showed a similar trend with experiment. In the future, model updating will be conducted to improve the reproducibility by the FEA.

References

- Cavell, D. and Waldron, P. 2001. A residual strength model for deteriorating post-tensioned concrete bridges. *Computers and Structures*, 79(4), 361-373.
- Dammika, A. J., Sheharyar, R., Takanami, R., Yamaguchi, H. and Matsumoto, Y. 2015. An investigation on modal damping ratio as an indicator of invisible damage in PC bridges. In: *Life-Cycle of Structural Systems: Design, Assessment, Maintenance and Management*, 404-410.
- Dilena, M. and Morassi, A. 2001. Dynamic testing of a damaged bridge. *Mechanical Systems and Signal Processing*, 25(5), 1485-1507.
- Dilena, M., Morassi, A. and Perin, M. 2001. Dynamic identification of a reinforced concrete damaged bridge. *Mechanical Systems and Signal Processing*, 25(8), 2990-3009.
- Döhler, M., Hille, F., Mevel, L., and Rucker, W. 2014. Structural health monitoring with statistical methods during progressive damage test of S101 Bridges. *Engineering Structures*, 69, 183-193.
- Kato, M. and Shimada, S. 1986. Vibration of PC bridge during failure process. *Journal of Structural Engineering*, 112(7), 1692-1703.
- Luna Vera, Oscar, Oshima, Y. and Kim, C.W. 2020. Flexural performance correlation to natural bending frequencies of post-tensioned concrete beams – Experimental investigation, *Journal of Civil Structural Health Monitoring*, 10(1), 135–151.
- Quattorone, A., Matta, E. Zanotti Fragonara, L., Ceravolo, R and De Stefano, A. 2012. Vibration tests on dismantled bridge beams and effects of deterioration. *Journal of Physics*, Conference Series 382 012059.
- Saiidi, M., Douglas, B. and Feng, S. 1994. Prestress force effect on vibration frequency of concrete bridges. *Journal of Structural Engineering*, 120(7), 2233-2241.
- Udwadia, F. E. 2005. Structural identification and damage detection from noisy modal data. *Journal of Aerospace Engineering*, 18(3), 179-187.